dForms with Constant Discrete Gaussian Curvature

Nicolas Leduc[1,2,*], Cyril Douthe[1], Bernard Vaudeville[2], Simon Aubry[2], Karine Leempoels[3], Laurent Hauswirth[4], Olivier Baverel[1,5]

[1] Laboratoire Navier, Ecole des Ponts, Univ. Eiffel, CNRS, 6-8, av. B. Pascal, 77455 France

[*] Corresponding author e-mail: nicolas.leduc@enpc.fr

[2] T/E/S/S atelier d'ingénierie, 7, cité Paradis, 75010 Paris, France

[3] Viry, 5, ZI de la Plaine - Eloyes, 88214 Remiremont Cedex, France

[4] Laboratoire d'Analyse et de Mathématiques Appliquées, Univ. Gustave Eiffel
5, boulevard Descartes, 77454 Marne-la-Vallée cedex 2, France

[5] École Nationale Supérieure d'Architecture de Grenoble
60, avenue de Constantine, 38000 Grenoble, France

Abstract

This paper proposes to extend the notions of mean and Gaussian curvatures of smooth and discrete surfaces to semi-discrete surfaces. This class of surfaces, also called piecewise developable surfaces is characterized by a zero Gaussian curvature everywhere except for seams between two patches and vertices. The study focuses on families of surfaces with constant Gaussian curvature along the seams. As a case study of the problem, dForms, closed piecewise developable surfaces formed by two discs of different shapes but equal perimeters, are chosen.

After a topological description of the semi-discrete surfaces, based on the Gauss-Bonnet theorem, two types of dForms with constant Gaussian curvature are studied. The first type describes a two-parameter family based on symmetrical cutting patterns. The symmetry property allows the three-dimensional geometry of this subclass of dForms to be fully described. The second type is asymmetrical and makes use of the properties of the evolute of the curves of the cutting patterns to fulfil the closure condition. In this case, we also propose a method to explore the space of possible configurations using an augmented isometric flow method.

Keywords: Piecewise developable surfaces, dForms, Steiner formula, Gaussian curvature, Gauss-Bonnet formula, Piecewise circular curve, Isometric flow.

1 Introduction

Differential geometry has been used for two centuries to describe smooth curves and surfaces locally. Much more recently, numerous research has been carried out to define equivalent notions for meshes using discrete differential geometry (Bobenko et al. 2008). Halfway between these theories, semi-discrete geometry, consisting of a patching of developable surfaces, has been widely explored in particular for constructive reasons. Its property of being isometric to the Euclidean plane makes it particularly relevant for forming complex three-dimensional objects from standard flat elements (sold in sheets or coils). Much of the effort has been focused on improving the approximation quality of complex surfaces, whether for cladding panels (Pottmann et al. 2008) or support structures (Tang et al. 2016). The seams between surfaces have also received attention, in particular through the work of Carl (2017) where he proposes a theory of curvature for semi-discrete surfaces. It is also worth mentioning curved folding, which has been the subject of numerous publications (Kilian et al. 2008; Tachi and Epps 2011), as it is of interest for the manufacture of complex mechanical parts (Duncan and Duncan 1982), specific industrial processes (Boersma and Molenaar 1995) or active kinematics of architectural components (Vergauwen et al. 2013).

In this paper, we propose to focus on a more general type of assembly of developable surfaces than curved folding: the curved patching. The first one assembles two surfaces sharing the same unrolled edge while in the second case the edges have different geometries (curvatures) after unrolling while keeping identical lengths. With technological properties comparable to the folded geometries, seam forms as designated by Demaine and Price (2010) have the advantage of contain Gaussian curvature along their connecting edges, the quantity and distribution of which is well known to help improve the mechanical behaviour of structures.

The dForms, closed piecewise developable surfaces formed by two discs of possibly different shapes but equal perimeters(Wills 2006), provide an interesting case to study curved patching. Initially limited to the field of industrial design, an architectural experimentation at full scale (Leduc et al. 2019) demonstrated the mechanical interest of this family of surfaces, but also the technological advantages by simplifying building process and assembly details (**fig. 1**).

As the sphere and the Platonic polyhedra are geometric figures with constant Gauss curvature for smooth and discrete geometry, is it not legitimate to ask which equivalents have the same property for semi-discrete geometry?

In the first part we will give definitions of the Gaussian and mean curvatures localised in the seams of piecewise developable surfaces (called PDS for the remainder of the

document) based on Steiner's formula. In the second part we will link these local geometry definitions to the topology of PDS using the Gauss-Bonnet formula. Once this theoretical framework has been developed, we will study two types of dForms with constant Gaussian curvature. The first type, addressed in the third part, describes a family of two-parameter surfaces based on symmetrical cutting patterns. The symmetry condition allows us to fully describe the three-dimensional geometry of these special dForms. The second type, discussed in the fourth part, identifies dForms with asymmetric cutting patterns, generated from an initial configuration, by an augmented isometric flow method.

Figure 1: Full scale prototype exhibiting closed piecewise developable surfaces acting as shear components in a double-layer space structure.

2 Gaussian and mean curvatures of piecewise developable surfaces

2.1 Steiner's formula applied to piecewise developable surfaces

Let σ_t be the normal shift (offset) of a smooth surface σ along this normal vector $t.\overrightarrow{n}$. Then the area of σ_t is a quadratic polynomial in t (Steiner Formula):

$$A(\sigma_t) = A(\sigma) - 2tH(\sigma) + t^2K(\sigma) \tag{1}$$

where $K(\sigma) = \int_\sigma K dA$ and $H(\sigma) = \int_\sigma H dA$ are the total Gaussian and mean curvature of σ. The same definition was used by Bobenko et al. (2008) to define analogous notions of discrete Gaussian and mean curvatures. At a vertex p of a polyhedral surface σ, the angle defect is called the Gaussian curvature:

$$K(p) = 2\pi - \sum \alpha_i \tag{2}$$

where α_i are the angles between neighbouring edges sharing the point p.

At an edge e of a closed polyhedral surface σ, the mean curvature is defined by:

$$H(p) = \frac{1}{2}\theta(e)\ell(e) \tag{3}$$

where $\ell(e)$ is the length of the edge e and $\theta(e)$ is the angle between the normals of the adjacent faces sharing the edge e ($\theta(e) > 0$ in the convex case and $\theta(e) < 0$ otherwise).

Gaussian and mean curvatures are contained within different geometric entities for polyhedral surfaces: Gaussian curvature is localised in the vertices whereas mean curvature is localised in the edges. The faces have no curvature.

By analogy with discrete surfaces (**fig. 2**), we define the elements for PDS as follows: face as a single smooth developable surface, edge as the intersection of two faces (except for boundaries) and vertex as the intersection of at least three edges (except for corners).

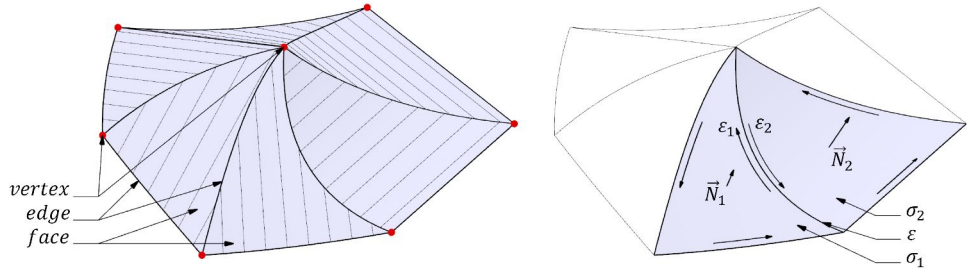

Figure 2: Piecewise developable surface: (**a**) terminology of the elements, (**b**) orientation and naming conventions.

In the case of PDS, we investigate the amount of Gaussian and mean curvatures localised within vertices, edges and faces (**fig. 3**).

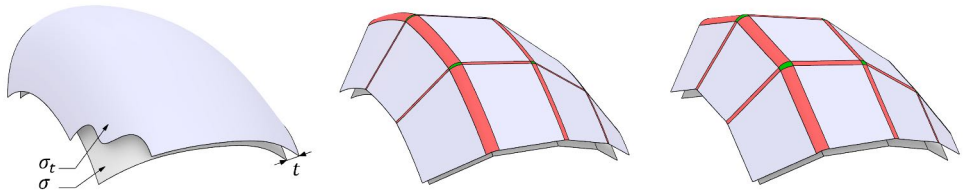

Figure 3: Steiner formula : illustration of the contribution for the Gaussian curvature of the faces (blue), edges (red) and vertices (green) in the case of : (**a**) smooth surfaces, (**b**) semi-discrete surfaces, (**c**) meshes.

Using an approach similar to that carried out on polyhedral surfaces, Gaussian curvature is defined at a vertex as the angular defect. The faces, being developable,

only have mean curvature and the total mean curvature corresponds to:

$$H(\sigma) = \int_{\sigma} H dA = \frac{1}{2} \int_{\sigma} \kappa_1 dA \tag{4}$$

where κ_1 is the non-zero principal curvature of σ.

The case of the edges is more delicate and a first qualitative indication is given by considering a PDS as the limit case of a one-directional refinement of a PQ mesh (Liu et al. 2006). In the direction of refinement, the edges and vertices merge into the seam curve which should contain the differential quantities localised in these elements, i.e. both Gaussian and mean curvature. In order to quantify these values, the problem can be approached by evaluating the area of the surface resulting from the offset of the curvilinear edges defined as a portion of pipe surface with the seam curve as its directrix.

Let p be a point located on the edge curve ε shared by the faces σ_1 and σ_2. The seam ε is called ε_1 (ε_2) when related to σ_1 (σ_2). The orientation of ε_1 and ε_2 is chosen counterclockwise according to the normals $\overrightarrow{N_1}$ and $\overrightarrow{N_2}$ (**fig. 2**); ε is oriented in the same way as ε_1. The curves ε_1 and ε_2 therefore have two opposite orientations.

Let the frames $F_{D_1}(p, \overrightarrow{T_{D_1}}, \overrightarrow{B_{D_1}}, \overrightarrow{N_{D_1}})$ and $F_{D_2}(p, \overrightarrow{T_{D_2}}, \overrightarrow{B_{D_2}}, \overrightarrow{N_{D_2}})$ be the Darboux frames along ε_1 and ε_2 on the surfaces σ_1 and σ_2. $F_F(p, \overrightarrow{T_F}, \overrightarrow{N_F}, \overrightarrow{B_F})$ is the Frenet frame of the curve ε. The angle θ_1 ($-\theta_2$) is then defined as the oriented angle between $\overrightarrow{N_F}$ and $\overrightarrow{N_{D_1}}$ ($\overrightarrow{N_{D_2}}$). The angular opening of the pipe surface of radius t is variable and equal to $\theta(p) = \theta_2 - \theta_1$ (see **fig. 4**).

The pipe can be locally approximated by a torus of minor radius t, the central circle of which is the osculating circle of the seam. The partial area of the torus is given by the formula:

$$A_{torus} = \int_{\varphi_1}^{\varphi_2} \int_{\theta_1}^{\theta_2} \left(tR + t^2 \cos\theta \right) \, d\theta d\varphi \tag{5}$$

where t is the minor radius of the torus and the value of the normal shift, R is the major radius of the torus and the radius of curvature of ε at p. θ describes the angular opening of A_{torus} along the minor circle and φ along the major circle.

The area measure dA_{torus} corresponding to the arc length measure of the seam curve $ds = Rd\varphi$ is derived from the previous formula:

$$dA_{torus} = \int_{\theta_1}^{\theta_2} \left(tR + t^2 \cos\theta \right) \, d\theta \, \frac{ds}{R} \tag{6}$$

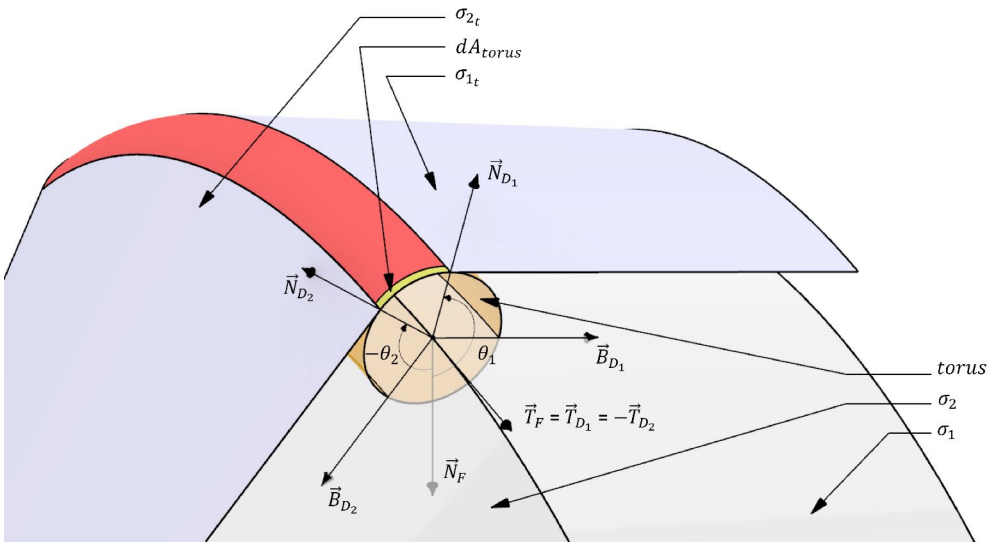

Figure 4: Definition of the Darboux and Frenet frames at point p of the seam.

$$dA_{torus} = \left(t[\theta_2 - \theta_1] + t^2 \left[\frac{\sin\theta_1}{R} - \frac{\sin\theta_2}{R} \right] \right) ds \tag{7}$$

By introducing κ_{g_1} and κ_{g_2}, geodesic curvatures of ε_1 and ε_1 at p:

$$dA_{torus} = \left(t[\theta_2 - \theta_1] + t^2[\kappa_{g_1} + \kappa_{g_2}] \right) ds \tag{8}$$

By identifying the linear and quadratic terms of Steiner's formula, the local Gaussian and mean curvatures in the seam are defined by:

$$K(p) = \kappa_{g_1}(p) + \kappa_{g_2}(p) \tag{9}$$

$$H(p) = \frac{1}{2}\theta(p) \tag{10}$$

2.2 Interpretation of the result

These definitions are fully compatible with the discrete case described above. For polyhedral surfaces, the geodesic curvature of the edges being zero, the Gaussian curvature is also zero at all points of the edges (**eq. (9)**). On the other hand, the constant angle between the local normals along the edge makes **eq. (10)** consistent with **eq. (3)**.

These formulas are also compatible with the well-known results of curved folding. Curved folds, like simple folds, has the property of being flattenable, implying a zero Gaussian curvature for any point on the faces or the fold. This is well confirmed by the **eq. (9)** since in the case of the curved folds, the geodesic curvatures have equal

and opposite values. Finally, we check the compatibility of the result with the one described in Pottmann and Wallner (2001): the osculating plane of the fold curve is the bisector plane of the two local tangent planes of the surfaces σ_1 and σ_2. The two tangent planes are described by the pairs of vectors $\left(\overrightarrow{T_{D_1}}, \overrightarrow{B_{D_1}}\right)$, $\left(\overrightarrow{T_{D_2}}, \overrightarrow{B_{D_2}}\right)$ and represented by angles $\beta_1 = \theta_1 - \frac{\pi}{2} = \left(\overrightarrow{N_F}, \overrightarrow{B_{D_1}}\right)$ and $\beta_2 = -\theta_2 - \frac{\pi}{2} = \left(\overrightarrow{N_F}, -\overrightarrow{B_{D_2}}\right)$. In the case of the curved folds, β_1 and β_2 are equal and opposite due to of the nullity of the quadratic term of **eq. (7)** involving:

$$\sin\theta_1 = sin\theta_2 \tag{11}$$

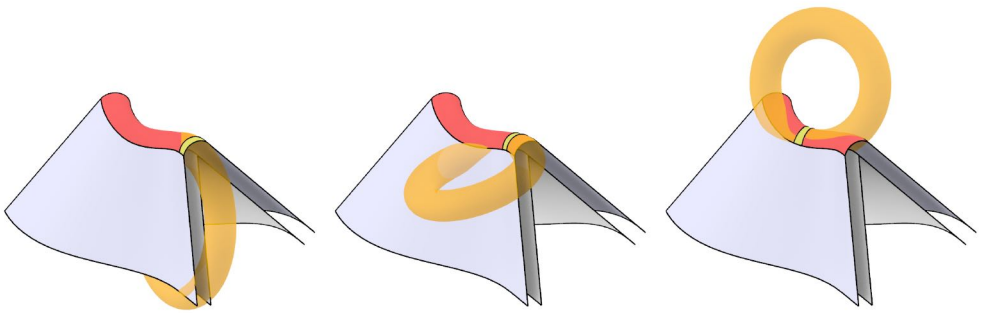

Figure 5: The three cases of Gaussian curvature whose sign is easily read by locating dA_{torus} on the osculating torus: (**a**) $K(p) > 0$, (**b**) $K(p) = 0$, (**c**) $K(p) < 0$.

3 Topologies of dForms

In differential geometry, the Gauss-Bonnet formula connects the geometry (in the sense of curvature) of a surface to its topology (in the sense of the Euler characteristic χ). In the simple case of a compact surface (without boundary), the formula is given by:

$$2\pi\chi = \int_{\sigma} K dA \tag{12}$$

In the case of piecewise smooth surfaces whose edges may themselves be piecewise smooth curves, the contribution of the edges and vertices of each piece should be considered. As recalled by Raffaelli et al. (2018), the Gauss-Bonnet formula for a patched surface made up of N_f faces called σ_i, N_{e_i} edges by faces σ_i called ε_{ij}, N_v vertices with N_{α_k} angles between neighbouring edges called α_{k_m} becomes:

$$\begin{aligned} 2\pi\chi &= \quad K_f \quad + \quad K_e \quad + \quad K_v \\ 2\pi\chi &= \sum_{i=1}^{N_f} \int_{\sigma_i} K dA + \sum_{i=1}^{N_f} \sum_{j=1}^{N_{e_i}} \int_{\varepsilon_{ij}} \kappa_g ds + \sum_{k=1}^{N_v} \left(2\pi - \sum_{m=1}^{N_{\alpha_k}} \alpha_{km}\right) \end{aligned} \tag{13}$$

where K_f, K_e, K_v are the total curvatures localised in the faces, edges and vertices, respectively. $\int_{\varepsilon_{ij}} \kappa_g ds$ is the total geodesic curvature of edge ε_{ij} on face σ_i.

In the specific case of piecewise developable surfaces, of interest here, the Gaussian curvature is zero at all points on the faces, which simplifies the previous formula by removing the first term from the **eq. (13)**.

We illustrate the Gauss-Bonnet formula applied to PDS by using the surface obtained by folding of the Vesica Piscis. This shape has the advantage of exhibiting simultaneously two vertices, two curved folding and one curved patching (**fig. 6**). The cutting pattern is formed by the intersection of two disks with the same radius, intersecting in such a way that the centre of each disk lies on the perimeter of the other (Fletcher 2004). Mundilova and Wills (2018) introduce an extra parameter in their study by modifying the distance d between the two centres. Excluding displacement and scale transformations, it is a parametric shape with one degree of freedom. With the variables as defined in **fig. 6**, it is easy to establish that:

$$\begin{aligned} \theta &= \gamma \\ L_1 = L_3 &= (2\pi - \theta)R \\ \ell_1 = \ell_{21} = \ell_{23} = \ell_3 &= \theta R \end{aligned} \tag{14}$$

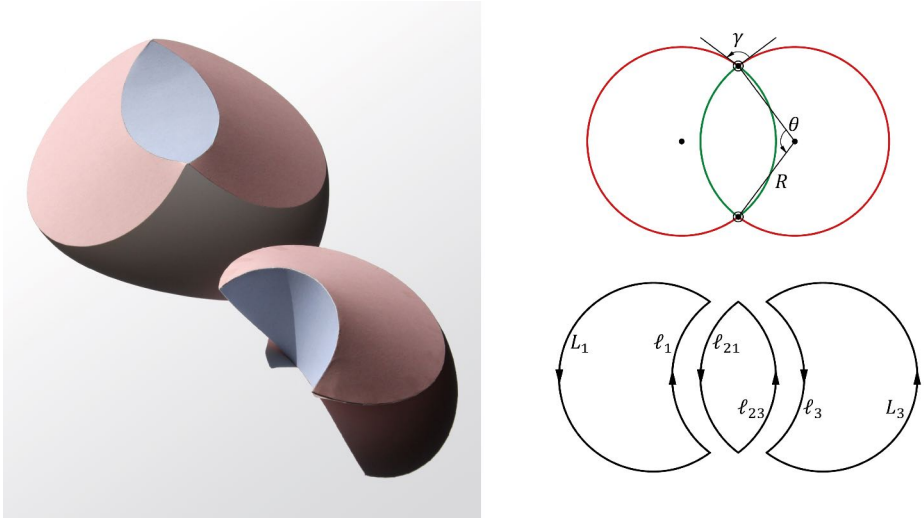

Figure 6: dForm based on the Vesica Piscis figure: (**a**) Physical model being assembled, (**b**) Cutting patterns showing the nature of the assemblies (point, fold (green), patch (red)) and naming conventions.

Taking into account the signed geodesic curvature of the cutting pattern curves, the three terms of the Gauss-Bonnet formula as defined in **eq. (13)** are:

$$\begin{aligned} K_f &= 0 \\ K_e &= \tfrac{1}{R}(L_1 + L_3) + \tfrac{1}{R}(\ell_{21} + \ell_{23}) - \tfrac{1}{R}(\ell_1 + \ell_3) = 2(2\pi - \theta) \\ K_v &= 2\theta \end{aligned} \tag{15}$$

By summing the three contributions, we obtain a constant value that is independent of the parameterization of the geometry: $K_f + K_e + K_v = 4\pi$, corresponding to a Euler characteristic $\chi = 2$ defining surfaces which are homeomorphic to a sphere.

Ghys (2014) analyses the Brazuca (official match ball of World cup 2014) as a polyhedron whose Gaussian curvature of the vertices has disappeared ($\sum \alpha_i = 2\pi$) and is distributed along the edges. Delp and Thurston (2011) propose, taking the Gauss-Bonnet relationship as a starting point, a generative method of shapes for an analogous distribution of the Gaussian curvature. In a similar way and based on the previously stated **eq. (9)**, we will study PDS with constant Gaussian curvature. This curvature is also exclusively contained in the seams, excluding shapes with vertices. For this reason, we limit our study to the case of dForms which are homeomorphic to a sphere and made up of two topological discs bounded by a curve of index 1. These shapes thus correspond to the simplified Gauss-Bonnet formula:

$$4\pi = \int_{\varepsilon} (\kappa_{g_1} + \kappa_{g_2}) ds \tag{16}$$

4 dForms with symmetrical cutting patterns

4.1 Two-parameter family of cutting patterns

A trivial case meets immediately the constraints outlined at the end of the previous part. It is a dForm made of two identical cutting patterns, a kind of developable tennis ball (see **fig. 7** and Cantat (2012)). Each cutting pattern is composed of two half-circles of radius R and two line segments, all four of identical length $\ell = \pi R$. With the arc facing the line segment, the Gaussian curvature $\kappa_{g_1} + \kappa_{g_2} = 1/R$ is constant and the resulting dForm consists of two half-cylinders with perpendicular axes and two half-disks. It directly satisfies the Gauss-Bonnet formula:

$$K(\sigma) = 4\ell(\kappa_{g_1} + \kappa_{g_2}) = 4\pi R \left(\frac{1}{R} + 0\right) = 4\pi \tag{17}$$

This type of cutting pattern with two distinct radii of curvature (among which one may be infinite as previously) can be generalized as a two-parameter family.

The two identical cutting patterns to be assembled are defined by a first discrete parameter N which characterizes the symmetry group to which they belong: the dihedral group D_N. The cutting patterns are thus made up of N symmetrical branches. A second continuous parameter α, defines the opening angle of the arc located at the end of the branch. A specific value of α for which the second arc has zero curvature separates two domains of convexity of the cutting patterns (see **fig. 8**).

Figure 7: Elementary dForm and cutting patterns consisting of half-circles and line segments.

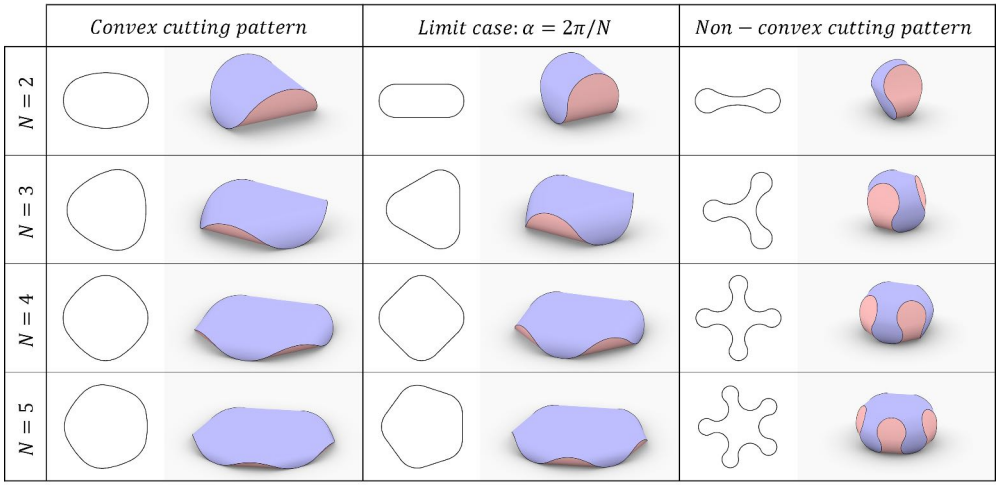

Figure 8: Double entry table showing the cutting patterns and corresponding dForms for values of $N = 2, 3, 4, 5$ and α with the three cases of convexity.

4.2 Parametrisation

Let $\mathcal{C}_{3d}$ be the seam curve of the dForm and $\mathcal{C}_{2d}$ the same developed curve on the xy plane. This latter curve defines the N-branch cutting pattern of the two parts to be assembled. Each curve is composed of $2N$ arcs: N identical arcs denoted $\mathcal{A}_{\alpha_i}$ alternating with N also identical arcs denoted $\mathcal{A}_{\beta_i}$ with $i \in \{0 \dots N-1\}$. The geometry of the arcs $(\mathcal{A}_{\alpha_i}, \mathcal{A}_{\beta_i})$ is defined by the three coupled parameters: opening angle (α, β), radius of curvature (R_α, R_β) and length $(\ell_\alpha = \alpha R_\alpha, \ell_\beta = \beta R_\beta)$. The curve $\mathcal{C}_{2d}$ being oriented counterclockwise, the angles and radii of curvature can be positive or negative depending on their own orientation compared to the orientation of $\mathcal{C}_{2d}$; with lengths that are always positive.

Figure 9 shows the example of arcs $\mathcal{A}_{\alpha_i}$ whose angle α and radius of curvature R_α are positive, the counterclockwise direction of the arc and the orientation of the curve $\mathcal{C}_{2d}$ being the same. On the other hand, β and R_β are negative in this configuration. The parameters of the arcs $\mathcal{A}_{\beta_i}$ are entirely defined from those of the arcs $\mathcal{A}_{\alpha_i}$. For assembly reasons, the lengths of the arcs ℓ_β are equal to ℓ_α. Furthermore, the closing condition with respect to the curvature of a curve of index 1 and length L expressed by the integral $\int_L \kappa ds = 2\pi$ corresponds in our case to $N(\alpha+\beta) = 2\pi$. The radius R_β can then be derived from the relation: $\ell_\beta = \beta R_\beta$

$$\begin{array}{rcl} \beta & = & \frac{2\pi}{N} - \alpha \\ R_\beta & = & R_\alpha \frac{\alpha}{\beta} = \frac{R_\alpha \alpha}{\frac{2\pi}{N} - \alpha} \\ \ell_\beta & = & \ell_\alpha \end{array} \tag{18}$$

The specific value of α introduced in the previous paragraph and defining the convexity of the cutting pattern is given for $R_\beta = \infty$ or $\beta = 0$, i.e. $\alpha = 2\pi/N$.

Figure 9 shows the cutting pattern in the coordinate system $(O_\alpha, \overrightarrow{x}, \overrightarrow{y})$ having as origin and x-axis the centre and axis of symmetry the first arc $\mathcal{A}_{\alpha_0}$. The positions of the centres O_{α_i}, O_{β_i} of the arcs $\mathcal{A}_{\alpha_i}$, $\mathcal{A}_{\beta_i}$ and O_D, the diedral centre of symmetry of the curve $\mathcal{C}_{2d}$, can then be determined by simple trigonometric relations. The coordinates of the first centre of the arcs $\mathcal{A}_{\alpha_0}$, $\mathcal{A}_{\beta_0}$ are given here, the others being derived by rotation of O_{α_0} and O_{β_0} by an angle $i\frac{2\pi}{N}$ around the point O_D.

$$\begin{array}{rcccl} O_{\alpha_0} & = & \begin{pmatrix} O_{\alpha_0 x} \\ O_{\alpha_0 y} \end{pmatrix} & = & \begin{pmatrix} 0 \\ 0 \end{pmatrix} \\ O_{\beta_0} & = & \begin{pmatrix} O_{\beta_0 x} \\ O_{\beta_0 y} \end{pmatrix} & = & \begin{pmatrix} (R_\beta - R_\alpha)\cos\frac{\alpha}{2} \\ (R_\beta - R_\alpha)\sin\frac{\alpha}{2} \end{pmatrix} \\ O_{\alpha_0} & = & \begin{pmatrix} O_{Dx} \\ O_{Dy} \end{pmatrix} & = & \begin{pmatrix} O_{\beta_0 x} - O_{\beta_0 y}\cot\frac{\pi}{N} \\ 0 \end{pmatrix} \end{array} \tag{19}$$

We check that the Gauss-Bonnet formula is well satisfied:

$$K(\sigma) = 2N\ell_\alpha \left(\frac{1}{R_\alpha} + \frac{1}{R_\beta}\right) = 2N\ell_\alpha \left(\frac{1}{R_\alpha} + \frac{R_\alpha \alpha}{\frac{2\pi}{N} - \alpha}\right) = 4\pi \tag{20}$$

The arc $\mathcal{A}_{\alpha_i}$ is parameterized in polar coordinates in the coordinate system $(O_{\alpha_i}, \overrightarrow{x}, \overrightarrow{y})$, see **fig. 9**. The point $p_{\tilde{\alpha}_i}(R_\alpha, \tilde{\alpha}_i)$ belongs to the arc $\mathcal{A}_{\alpha_i}$ and $\tilde{\alpha}_i$ represents the value of the angle $\left(\overrightarrow{x}, \overrightarrow{O_{\alpha_i} p_{\tilde{\alpha}_i}}\right)$. To this point located on the arc $\mathcal{A}_{\alpha_i}$ of the first cutting pattern corresponds a point $p_{\tilde{\beta}_i}(R_\beta, \tilde{\beta}_i)$ located on the arc $\mathcal{A}_{\beta_i}$ of the second cutting pattern with $\tilde{\beta}_i$ denoting the value of the angle

$\left(\overrightarrow{x}, \overrightarrow{O_{\beta_i} p_{\tilde{\beta}_i}}\right)$. The angles $\tilde{\alpha}_i$ and $\tilde{\beta}_i$ are in the range $[\alpha_{s_i}, \alpha_{e_i}]$ and $[\beta_{s_i}, \beta_{e_i}]$ of length α and β. The point p belonging to the seam of the dForm is the result of the identification of the points $p_{\tilde{\alpha}_i}$ and $p_{\tilde{\beta}_i}$. By virtue of the equality of the arc length at point $p = p_{\tilde{\alpha}_i} = p_{\tilde{\beta}_i}$, the relation $R_\alpha(\tilde{\alpha}_i - \alpha_{s_i}) = R_\beta(\tilde{\beta}_i - \beta_{s_i})$ implies:

$$\tilde{\beta}_i = \frac{R_\alpha}{R_\beta}(\tilde{\alpha}_i - \alpha_{s_i}) + \beta_{s_i} \tag{21}$$

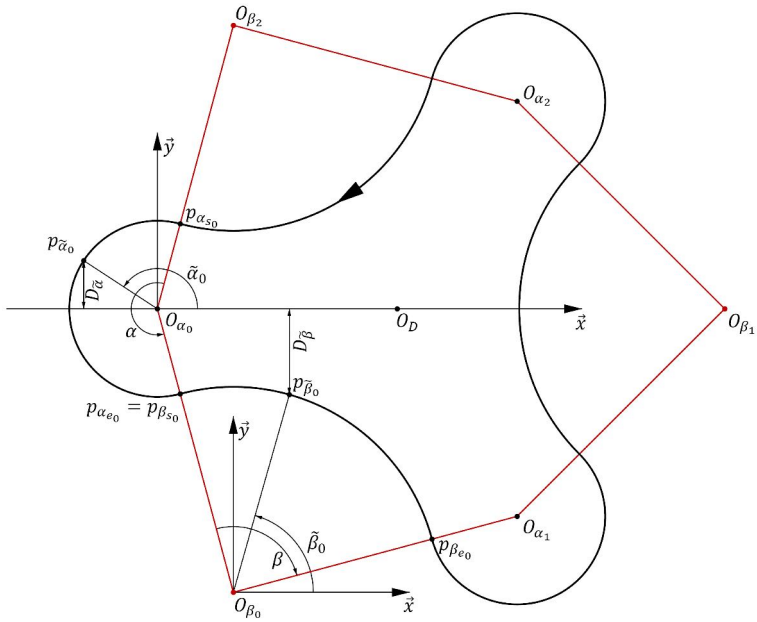

Figure 9: Angle and distance naming convention: cutting pattern for $N = 3$, $\alpha = \frac{7\pi}{6}$.

4.3 From 2d cutting pattern to dForm

The modelling of isometric deformation of flat shapes into three-dimensional surfaces is not a trivial exercise. The case of dForms is even more complicated due to the global nature of the problem, as pointed out by Pottmann and Wallner (2001).

At the present time, two different approaches can be identified in the literature. The first is based on optimization algorithms that minimize the energy contained in a triangular mesh, such as the Surface Evolver software (Brakke 2014) used by Paul Bourke (nd) to model dForms. The second approach is based on Alexandrov's theorem showing the existence of a convex polytope with a given metric on the boundary (Bobenko and Izmestiev 2008).

In our case, the symmetry conditions of the cutting patterns give us the possibility to fully describe the geometry of the three-dimensional shape.

Let us first consider the deformation kinematics of the planar cutting patterns to form the dForm in space (**fig. 10**). We denote $(O_{D_1}, \overrightarrow{x_1}, \overrightarrow{y_1}, \overrightarrow{z_1})$ and $(O_{D_2}, \overrightarrow{x_2}, \overrightarrow{y_2}, \overrightarrow{z_2})$ the two frames attached to the cutting patterns to be assembled. These two frames, linked by a screw motion, are located in a global coordinate system $(O, \overrightarrow{x}, \overrightarrow{y}, \overrightarrow{z})$ such that $O_{D_1}(0,0,-h)$, $\overrightarrow{z} = \overrightarrow{z_1}$, $(\overrightarrow{x}, \overrightarrow{x_1}) = -\frac{\pi}{2N}$ and $O_{D_2}(0,0,h)$, $\overrightarrow{z} = \overrightarrow{z_2}$, $(\overrightarrow{x}, \overrightarrow{x_2}) = \frac{\pi}{2N}$. Each point of a branch then moves in a plane parallel to its plane of symmetry and the developable surface of the branch takes the form of a general cylinder whose rulings remain parallel to the xy plane and perpendicular to the plane of symmetry.

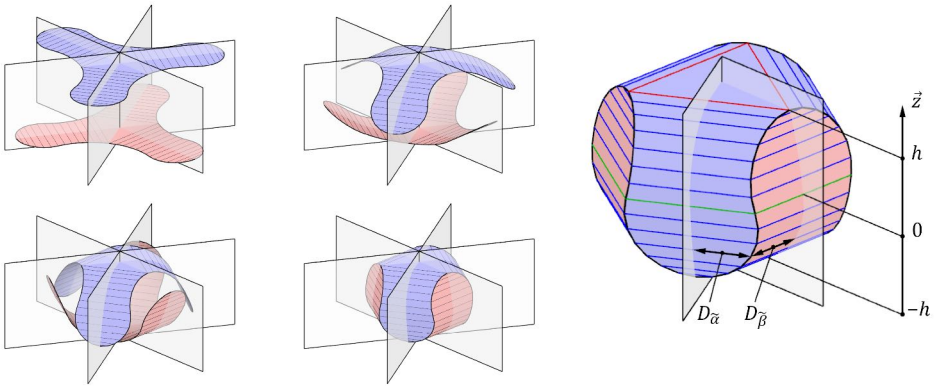

Figure 10: Symmetrical dForm: (**a**) Assembly kinematics of the dForm, (**b**) Visualization of the polygonal horizontal section: regular polygon (green), symmetrical polygon (D_N) (blue), degenerate polygon (red).

Let us now consider the dForm when assembled (**fig. 10**). Since all the rules are parallel to the xy plane, the intersection of a plane of equation $z = t$ with the dForm is a $2N$-sided polygon belonging to the dihedral symmetry group D_N, centered on the axis $(O, \overrightarrow{z})$. This polygon is regular for $t = 0$ and degenerates into a regular N-sided polygon for $t = \{-h, h\}$.

Describing the geometry of the dForm is therefore equivalent to determining the geometry of polygons and their position in space. The symmetry conditions indicate the position and rotation of these polygons in the plane $(O, \overrightarrow{x}, \overrightarrow{y})$. The remaining unknowns to be determined are the side lengths and the positioning of the polygons along the axis $(O, \overrightarrow{z})$.

The half-lengths of the sides of the polygons, i.e. the distance from point p to the planes of symmetry of the two branches to which p belongs, can be measured

directly on the cutting patterns. For symmetry reasons, it is only necessary to consider the first arcs $\mathcal{A}_{\alpha_0}$ and $\mathcal{A}_{\beta_0}$.

$$\begin{array}{rcl} D_{\tilde{\alpha}} & = & R_\alpha \sin\tilde{\alpha}_0 \\ D_{\tilde{\beta}} & = & -O_{\beta_0 y} - R_\beta \sin\tilde{\beta}_0 \end{array} \tag{22}$$

$D_{\tilde{\alpha}}$ and $D_{\tilde{\beta}}$ are always positive, according to the sign conventions for radii and angles (e.g. in **fig. 9**, $O_{\beta_0 y} < 0$ and $R_\beta < 0$).

Knowing the planes of symmetry of the polygon, it is possible to determine the coordinates p_x and p_y of point p in the plane $(O, \overrightarrow{x}, \overrightarrow{y})$. To determine the p_z coordinate, we rely on the preservation of the arc length parameterization $s(\tilde{\alpha})$ of the curve (isometric deformation) which is given by:

$$s(\tilde{\alpha}) = \int_{\alpha_s}^{\tilde{\alpha}} ds = R_\alpha(\tilde{\alpha} - \alpha_s) \tag{23}$$

The above considerations imply $z'(s)^2 = 1 - x'(s)^2 - y'(s)^2$ and the symmetry of the shape makes it possible to bound the angle domain to $\tilde{\alpha}_0 \in [\alpha_{s_0}, \pi]$.

$$p(p_x, p_y, p_z) = \begin{pmatrix} D_{\tilde{\alpha}} \\ \frac{1}{\sin\frac{\pi}{N}} D_{\tilde{\beta}} + \cot\frac{\pi}{N} D_{\tilde{\alpha}} \\ \int_{\alpha_s}^{\tilde{\alpha}} \sqrt{1 - x'(s)^2 - y'(s)^2} ds \end{pmatrix} \tag{24}$$

With $\bar{\alpha}$ as the variable of integration:

$$\begin{array}{rcl} ds & = & R_\alpha \; d\bar{\alpha} \\ dx & = & R_\alpha \cos\bar{\alpha} \; d\bar{\alpha} \\ dy & = & \frac{R_\alpha}{\sin\frac{\pi}{N}} \left[\cos\frac{\pi}{N}\cos\bar{\alpha} - \cos\bar{\beta}\right] \; d\bar{\alpha} \end{array}$$

From a discrete point of view, the seam curve can be considered as a polygonal curve resulting from the isometric deformation of the cutting patterns. Each arc $\mathcal{A}_{\alpha_i}$ and $\mathcal{A}_{\beta_i}$ is subdivided into n arcs of equal length; subdivision points are denoted p_{α_k} and p_{β_k} with $k = \{0 \ldots n\}$. Corresponding points on the discrete seam of the dForm are denoted $p_k(p_{k_x}, p_{k_y}, p_{k_z})$.

In a similar way to the continuous approach, the values p_{k_x} and p_{k_y} are determined directly from the cutting patterns. The coordinate p_{k_z} is calculated by discrete integration, the initial position of the point p_0 on the median plane $(z = 0)$ being known. For a sufficiently fine discretization, we can consider in a first-order approximation that the length of the arc $(p_{k-1}p_k) = \frac{R_\alpha \alpha}{n}$. The point p_k is thus at

the intersection of the sphere $\mathcal{S}\left(p_{k-1}, \frac{R_\alpha \alpha}{n}\right)$ with the planes $x = p_{k_x}$ and $y = p_{k_y}$. The point p_k therefore has the coordinates:

$$p_k(p_{k_x}, p_{k_y}, p_{k_z}) = \begin{pmatrix} D_{\alpha_k} \\ \frac{1}{\sin\frac{\pi}{N}} D_{\beta_k} + \cot\frac{\pi}{N} D_{\alpha_k} \\ \sqrt{\left(\frac{R_\alpha \alpha}{n}\right)^2 - (p_{k_x} - p_{(k-1)_x})^2 - (p_{k_y} - p_{(k-1)_y})^2} + p_{(k-1)_z} \end{pmatrix} \tag{25}$$

4.4 Curvature and torsion of the seam curve

We saw in the previous paragraph that it is possible to formulate the parametric equation of $\mathcal{C}_{3d}$ as a Rieman integral. However, the differential properties of this curve can be expressed explicitly by proceeding to the successive derivatives of eq. (24). Taking the convention $\dot{\mathcal{C}}_{3d} = \frac{dp}{ds}$, $\ddot{\mathcal{C}}_{3d} = \frac{d^2p}{ds^2}$, $\dddot{\mathcal{C}}_{3d} = \frac{d^3p}{ds^3}$ and since the curves $\mathcal{C}_{2d}$ and $\mathcal{C}_{3d}$ are parameterized by arc length, the curvature and torsion of the curves are defined by Do Carmo (1976):

$$\begin{aligned} \kappa &= \|\ddot{\mathcal{C}}_{3d}\| \\ \tau &= \frac{(\dot{\mathcal{C}}_{3d} \wedge \ddot{\mathcal{C}}_{3d}) \cdot \dddot{\mathcal{C}}_{3d}}{\kappa^2} \end{aligned} \tag{26}$$

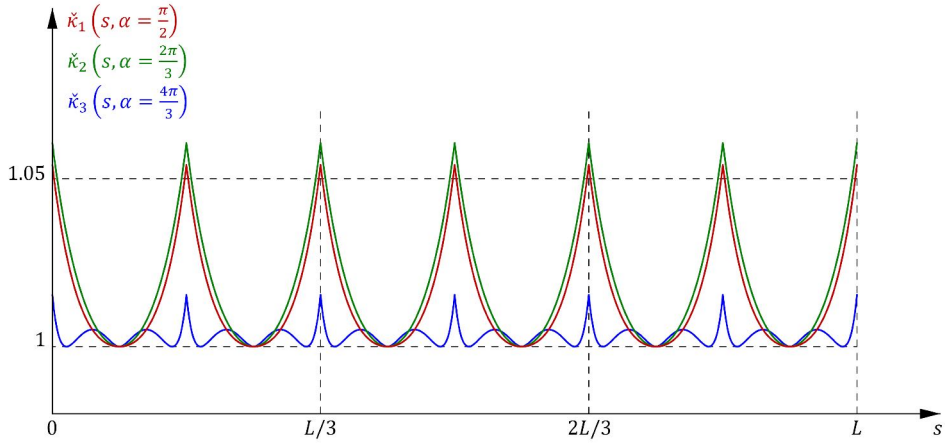

Figure 11: Curvature of the seam curve as a function of the arc length.

The details of the calculations in our case are not given here, but the graphs of the curvature as a function of the arc length of the seam (origin taken at p_0) are given for three different dForms $\left(N = 3 \text{ and } \alpha_j = \left\{\frac{\pi}{2}, \frac{2\pi}{3}, \frac{4\pi}{3}\right\} \text{ for } j = 1,2,3\right)$ in fig. 11. These three angles represent the convex, limit and non-convex cases. It should be noted that in order to superimpose the three graphs, we consider the

value $\check{R}_{\alpha_j} = \frac{R_{\alpha_j}}{\ell_{\alpha_j}}$ to normalize the length of the arcs: $\ell_{\alpha_j} = \ell_{\beta_j} = 1$. Similarly, the displayed value of the curvature $\check{\kappa}_j$ is normalized by the radius of the arc $\mathcal{A}_{\alpha_j}$: $\check{\kappa}_j = \kappa_j \cdot \check{R}_{\alpha_j}$

5 dForms with dissymmetrical cutting patterns

5.1 General description of the process

Without pretending to describe them exhaustively, we aim to identify some dForms whose seams have constant Gaussian curvature and their cutting pattern curves are neither identical nor symmetrical. As before, these are made up of arcs with tangential continuity, often referred to in the literature as Piecewise Circular Curves (PCC).

Let $\mathcal{C}_1$ be the boundary curve of the first cutting pattern. It consists of n arcs of circles $\mathcal{A}_{1_i}$ defined by the three coupled parameters $(\alpha_{1_i}, R_{1_i}, \ell_{1_i})$. As before, angles and radii of curvatures are defined algebraically according to their orientation with respect to the counter-clockwise orientation of the curve. The curve $\mathcal{C}_2$ of the second cutting pattern, which also consists of n arcs of circles $\mathcal{A}_{2_i}$ with parameters $(\alpha_{2_i}, R_{2_i}, \ell_{2_i})$) is then completely defined by the parameters of the first curve: the lengths of the arcs are in equal pairs to enable the cutting patterns to be assembled and the radii of curvature are determined by the constant Gaussian curvature constraint.

The difficulty of this exercise lies mainly in the global problem of satisfying the simultaneous closure in position and tangency of the two curves $\mathcal{C}_1$ and $\mathcal{C}_2$. For this purpose, we investigate the properties of the evolute of PCCs on which we will impose conditions ensuring the closure of the related curve.

5.2 Piecewise circular curves and evolute

The evolute of a curve, the locus of all its centres of curvature is redefined by Banchoff and Giblin (1994) in the case of the PCCs: the evolute is the polygonal curve connecting the centres of the circular arcs.

Let c_i be the center of the arc $\mathcal{A}_i$ (also the corresponding vertex of the evolute). The connecting point between arcs $\mathcal{A}_i$ and $\mathcal{A}_{i+1}$, denoted p_i, is located on the support line of the edge $\mathcal{E}_i$ of the evolute connecting the centres c_i and c_{i+1}. The tangency condition between two consecutive arcs implies that the length of the vector $\overrightarrow{e_1} = \overrightarrow{c_i c_{i+1}}$ corresponding to the edge $\mathcal{E}_i$ is directly related to the radii of the arcs of circles $\mathcal{A}_i$ and $\mathcal{A}_{i+1}$, more precisely, $\|\overrightarrow{e_1}\| = |R_{i+1} - R_i| = |\ell_{e_i}|$ with ℓ_{e_i} defined as the signed length of $\mathcal{E}_i$. The rotating angle between the vectors $\overrightarrow{e_i}$ and $\overrightarrow{e_{i+1}}$ is denoted α_{e_i}.

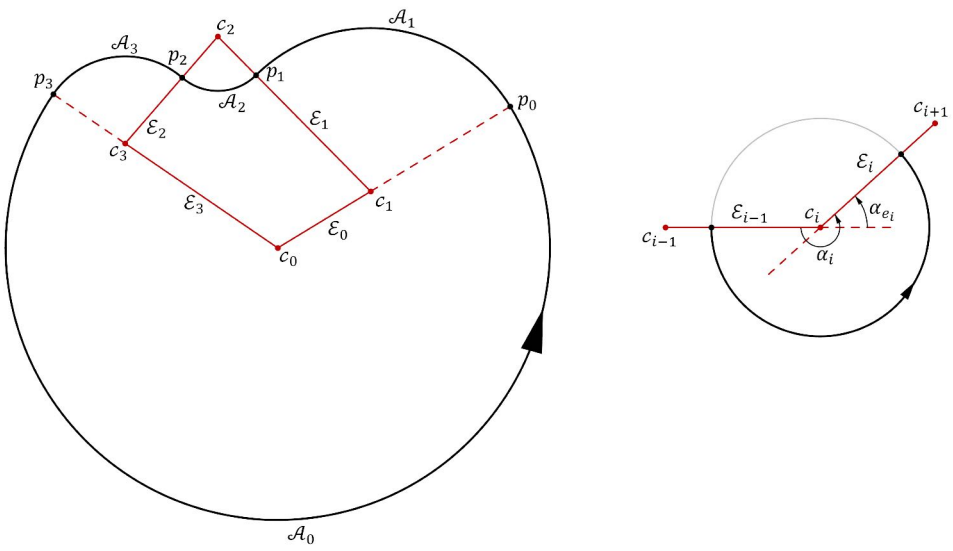

Figure 12: Naming convention: (**a**) PCC and related evolute, (**b**) Angles definition.

We are now considering the conditions on the evolute to ensure the closure in position and tangency of the related PCC. Given the definition of the evolute of a PCC, any closed PCC has a closed polygonal evolute, which is the first condition for closure.

In addition, we saw previously that for any pair of arcs $\mathcal{A}_i$ and $\mathcal{A}_{i+1}$ connected in tangency, the signed length of the evolute is given by $\ell_{e_i} = R_{i+1} - R_i$. In particular, for the side $\mathcal{E}_{n-1}$ which closes the evolute, $\ell_{e_{n-1}} = R_0 - R_{n-1}$. The zero telescopic sum of the signed lengths gives the second closing condition, summarized with the first one as:

$$\begin{aligned} \sum_{i=0}^{n-1} \overrightarrow{e_i} &= \overrightarrow{0} \\ \sum_{i=0}^{n-1} \ell_{e_i} &= 0 \end{aligned} \tag{27}$$

5.3 Generative process

The process of generating solution families of non-symmetric but constant Gaussian curvature dForms is a two-step process. An initial solution is generated first by optimization. A geometrical flow is then applied that satisfies both the constant Gaussian curvature constraint and the closure conditions of the two PCCs.

The first cutting pattern $\mathcal{C}_1$ is arbitrarily generated from a closed smooth curve approximated by biarcs (Piegl and Tiller 2002). This technique guarantees a connection in position and tangency between the n arcs $\mathcal{A}_{1_i}(\alpha_{1_i}, R_{1_i}, \ell_{1_i})$.

The second cutting pattern $\mathcal{C}_2$ is generated by computing the parameters of the n arcs $\mathcal{A}_{2_i}(\alpha_{2_i}, R_{2_i}, \ell_{2_i})$ from $\mathcal{A}_{1_i}$. According to the **eq. (9)**, $K = \kappa_{1_i} + \kappa_{2_i}$, where K is the Gaussian curvature, κ_{1_i} and κ_{2_i} are the curvatures of the arcs $\mathcal{A}_{1_i}$ and $\mathcal{A}_{2_i}$. Since the Gaussian curvature is constant and entirely contained in the seam, it is derived from the Gauss-Bonnet formula: $K = \frac{4\pi}{L}$ with $L = \sum \ell_i$.

$$\begin{aligned} \ell_{2_i} &= \ell_{1_i} \\ R_{2_i} &= \frac{1}{K - \kappa_{1_i}} \\ \alpha_{2_i} &= \alpha_{1_i}\left(\frac{K}{\kappa_{1_i}} - 1\right) \end{aligned} \tag{28}$$

In the general case, the concatenation of the computed arcs $\mathcal{A}_{2_i}$ yields an open curve $\mathcal{C}_2$. By applying the closure conditions given in **eq. (27)** on the related evolutes of curves $\mathcal{C}_1$ and $\mathcal{C}_2$, it is possible to close them by constrained optimization.

The formulae for the closing conditions of a PCC indicate that they depend only on the relationship between the signed lengths of the sides of the evolute and the difference in the radii of the arcs, independently of the turning angles, provided that the evolute remains closed. It indicates that we can consider the evolute as a closed rigid bar linkage whose joints are the centres of discs that "roll" on each other. The PCC supported by these discs remains closed regardless of the deformation of this mechanism (**fig. 13**).

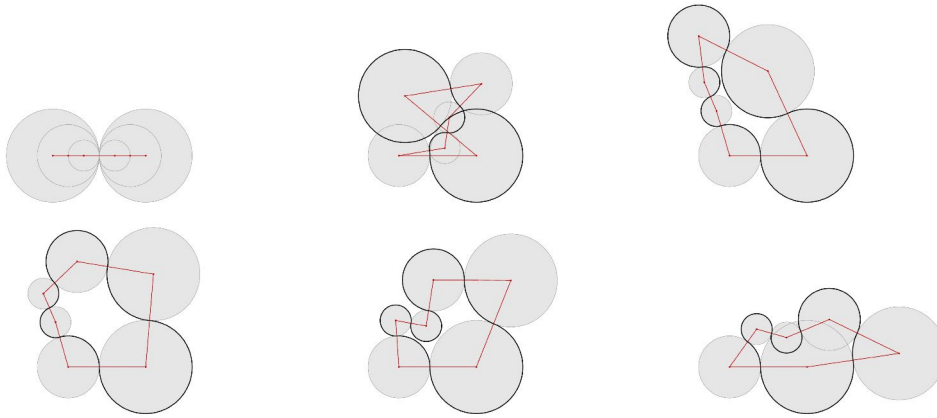

Figure 13: The isometric deformation of the evolution preserves the closure of the related PCC.

This type of deformation is obtained by the application of an isometric flow that maintains, over time, the length of a curve and its closure whilst modifying its geometry (its curvature). The constraints related to this type of flow are described for a continuous curve by Crane et al. (2013).

In the case of a polygonal curve that we consider here, the constraints become:

$$\langle \dot{\alpha}_{e_i}, \mathbb{1} \rangle = \langle \dot{\alpha}_{e_i}, c_{i_x} \rangle = \langle \dot{\alpha}_{e_i}, c_{i_y} \rangle = 0 \tag{29}$$

where $\langle . \rangle$ is the scalar product, $\dot{\alpha}_{e_i} = \frac{d\alpha_{e_i}}{dt}$ is the time derivative of the turning angle, c_{i_x} and c_{i_y} are the coordinates of the vertices of the evolute.

The isometric flow applied to the evolute of the curve $\mathcal{C}_1$ guarantees that the closure of the first cutting pattern is preserved but is not sufficient to ensure the closure of the curve $\mathcal{C}_2$. It is therefore necessary to increase the constraints of the isometric flow applied to the first cutting pattern by integrating the closure conditions of curve $\mathcal{C}_2$ by passing them through the relations defined in **eq. (28)**. The implementation of this augmented isometric flow does not present any additional theoretical issues (see the example of **fig. 14**). However, the study of the general problem requires the description of numerous bifurcations which make an exhaustive description of it inappropriate here.

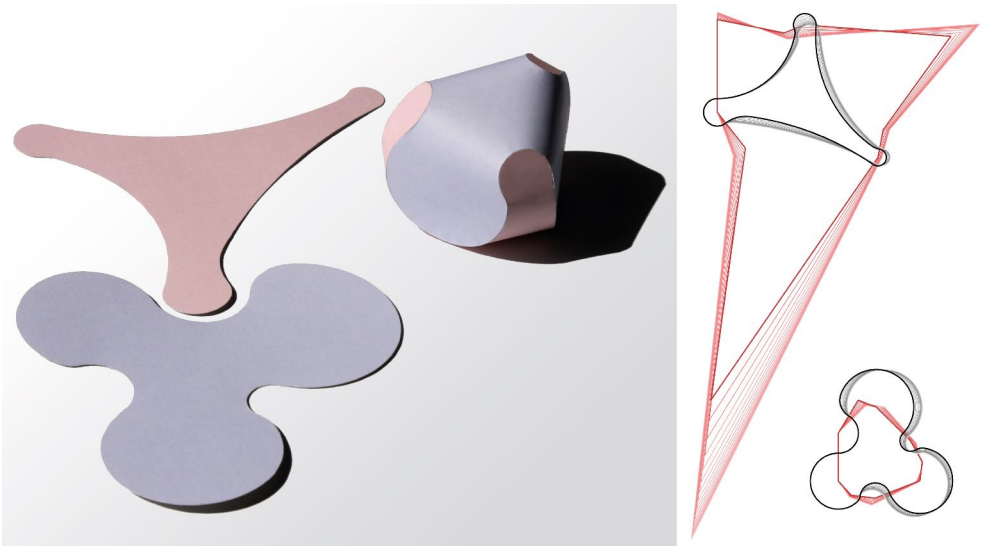

Figure 14: Dissymmetrical dForm: (**a**) Initial configuration (physical model), (**b**) Family of cutting patterns and evolutes generated by augmented isometric flow.

6 Conclusions and further work

By locating and quantifying the differential properties in the seams of piecewise developable surfaces, we have highlighted the existence of shapes, symmetrical or not, with the particularity of having a constant Gaussian curvature. Even if the applications do not seem immediate, this work should be considered as a preliminary step towards a better control of the distribution of the Gaussian curvature within shell structures covered with developable panels.

To further develop this hybrid design combining constructive rationality and structural efficiency, the model will have to integrate more geometric components to consider various architectural and technical constraints. The first ideas to be explored are to increase the number of patched surfaces and to apply these principles to an open boundary. Finally, acting on the Gaussian curvature itself by optimizing a prescribed curvature rather than a constant curvature or by introducing non-zero Gaussian curvature vertices should make it possible to significantly improve structural behaviour.

Acknowledgements

This research was supported by Navier lab., TESS atelier d'ingénerie and VIRY Fayat group, partners of the CIFRE thesis "Building with developable surfaces".

References

Banchoff, T. and P. Giblin (1994). On the geometry of piecewise circular curves. *The American Mathematical Monthly 101*(5), 403–416.

Bobenko, A. and I. Izmestiev (2008). Alexandrov's theorem, weighted Delaunay triangulations, and mixed volumes. *Annales de l'institut Fourier 58*(2), 447–505.

Bobenko, A. I., P. Schröder, J. M. Sullivan, and G. M. Ziegler (2008). *Discrete Differential Geometry*. Birkhäuser.

Boersma, J. and J. Molenaar (1995). Geometry of the shoulder of a packaging machine. *Siam Review 37*(3), 406–422.

Bourke, P. (n.d.). dforms. `http://paulbourke.net/geometry/dform/`.

Brakke, K. A. (2014). Surface Evolver. `http://facstaff.susqu.edu/b/brakke/evolver/evolver.html`.

Cantat, S. (2012, August). La balle et la courbe. `https://images.math.cnrs.fr/La-balle-et-la-courbe.html`.

Carl, W. (2017). On semidiscrete constant mean curvature surfaces and their associated families. *Monatshefte für Mathematik 182*(3), 537–563.

Crane, K., U. Pinkall, and P. Schröder (2013). Robust fairing via conformal curvature flow. *ACM Transactions on Graphics (TOG) 32*(4), 1–10.

Delp, K. and B. Thurston (2011). Playing with Surfaces: Spheres, Monkey Pants, and Zippergons. In *Proceedings of Bridges 2011: Mathematics, Music, Art, Architecture, Culture*, pp. 1–8. Tessellations Publishing.

Demaine, E. D. and G. N. Price (2010). Generalized D-Forms Have No Spurious Creases. *Discrete & Computational Geometry 43*(1), 179–186.

Do Carmo, M. (1976). *Differential geometry of curves and surfaces*. Prentice Hall.

Duncan, J. P. and J. L. Duncan (1982). Folded Developables. *Proceedings of the Royal Society of London. Series A, Mathematical and Physical Sciences 383*(1784), 191–205.

Fletcher, R. (2004). Musings on the Vesica Piscis. *Nexus network journal 6*(2), 95–110.

Ghys, E. (2014). Le Brazuca, le ballon cubique de la coupe du monde. `https://images.math.cnrs.fr/Le-Brazuca-le-ballon-cubique-de-la-Coupe-du-monde.html`.

Kilian, M., S. Flöry, Z. Chen, N. J. Mitra, A. Sheffer, and H. Pottmann (2008). Curved folding. *ACM transactions on graphics (TOG) 27*(3), 1–9.

Leduc, N., C. Douthe, G. Hivin, B. Vaudeville, S. Aubry, K. Leempoels, and O. Baverel (2019). Space Structure with Developable Shear Components. In *Proceedings of the International fib Symposium on Conceptual Design of Structures*, Spain, pp. 345–352.

Liu, Y., H. Pottmann, J. Wallner, Y.-L. Yang, and W. Wang (2006). Geometric modeling with conical meshes and developable surfaces. *ACM Transactions on Graphics (TOG) 25*(3), 681–689.

Mundilova, K. and T. Wills (2018). Folding the Vesica Piscis. In *Bridges 2018 Conference Proceedings*, pp. 535–538. Tessellations Publishing.

Piegl, L. A. and W. Tiller (2002, September). Biarc approximation of NURBS curves. *Computer-Aided Design 34*(11), 807–814.

Pottmann, H., A. Schiftner, P. Bo, H. Schmiedhofer, W. Wang, N. Baldassini, and J. Wallner (2008). Freeform surfaces from single curved panels. *ACM Transactions on Graphics (TOG) 27*(3), 1–10.

Pottmann, H. and J. Wallner (2001). *Computational line geometry*. Springer Science & Business Media.

Raffaelli, M., J. Bohr, and S. Markvorsen (2018). Cartan ribbonization and a topological inspection. *Proceedings of the Royal Society A 474*(2220), 20170389.

Tachi, T. and G. Epps (2011). Designing One-DOF mechanisms for architecture by

rationalizing curved folding. In *International Symposium on Algorithmic Design for Architecture and Urban Design (ALGODE-AIJ). Tokyo*, Volume 5, pp. 6.

Tang, C., M. Kilian, P. Bo, J. Wallner, and H. Pottmann (2016). Analysis and design of curved support structures. In *Advances in Architectural Geometry*, pp. 8–22.

Vergauwen, A., L. Alegria Mira, K. Roovers, and N. De Temmerman (2013). Parametric design of adaptive shading elements based on Curved-line Folding. In *Proceedings of the First Conference Transformables 2013*.

Wills, T. (2006). DForms: 3D forms from two 2D sheets. In *Bridges: Mathematical Connections in Art, Music, and Science*, pp. 503–510.